

Stochastic Aspects of Oscillatory Ca^{2+} Dynamics in Hepatocytes

Geneviève Dupont,* Aurélie Abou-Lovergne,^{†‡} and Laurent Combettes^{†‡}

*Unité de Chronobiologie Théorique, Université Libre de Bruxelles, Faculté des Sciences, B-1050, Brussels, Belgium; and [†]Institut National de la Santé et de la Recherche Médicale, UMR-S757, [‡]Université Paris-Sud, F-91405 Orsay, France

ABSTRACT Signal-induced Ca^{2+} oscillations have been observed in many cell types and play a primary role in cell physiology. Although it is the regular character of these oscillations that first catches the attention, a closer look at time series of Ca^{2+} increases reveals that the fluctuations on the period during individual spike trains are far from negligible. Here, we perform a statistical analysis of the regularity of Ca^{2+} oscillations in norepinephrine-stimulated hepatocytes and find that the coefficient of variation lies between 10% and 15%. Stochastic simulations based on Gillespie's algorithm and considering realistic numbers of Ca^{2+} ions and inositol trisphosphate (InsP_3) receptors account for this variability if the receptors are assumed to be grouped in clusters of a few tens of channels. Given the relatively small number of clusters (~ 200), the model predicts the existence of repetitive spikes induced by fluctuations (stochastic resonance). Oscillations of this type are found in hepatocytes at subthreshold concentrations of norepinephrine. We next predict with the model that the isoforms of the InsP_3 receptor can affect the variability of the oscillations. In contrast, possible accompanying InsP_3 oscillations have no impact on the robustness of signal-induced repetitive Ca^{2+} spikes.

INTRODUCTION

Signal-induced Ca^{2+} oscillations are observed in cells of various types and are known to play a primary role in transducing the external signal into the appropriate physiological response (1). Given the large number of physiological processes that are controlled by inositol trisphosphate (InsP_3)-induced Ca^{2+} increases, these signals are highly organized in time and space to ensure reliability and specificity (2–4). To mention only a few examples, oscillations and waves have indeed been observed in cells as various as eggs (5), cardiac myocytes (6), astrocytes (7), and plant cells (8). The nature and intensity of the external signal are encoded in the frequency, amplitude, or waveform of Ca^{2+} oscillations (9,10). Given the widespread relevance of frequency encoding in Ca^{2+} dynamics, the issue of the regularity of oscillations, as that observed for many other biological rhythms (11), is of great conceptual and physiological interest.

Experimental and theoretical studies, however, show that randomness plays a key role in Ca^{2+} dynamics. At low stimulation levels, Ca^{2+} increases of small amplitude (~ 100 nM), duration (~ 100 ms), and spatial extent ($1\text{--}3\ \mu\text{m}$) have been observed, especially in HeLa cells (12) and *Xenopus* oocytes (13). Given the small numbers of InsP_3 receptors (InsP_3Rs) and Ca^{2+} ions taking part in these elementary events, the so-called Ca^{2+} “blips” and “puffs” occur randomly. However, their frequency, amplitude, and duration increase with InsP_3 concentration. For suprathreshold levels of stimulation, these Ca^{2+} increases do not remain localized but propagate as intracellular waves. At the same time, Ca^{2+}

signals repeat regularly in time and can thus be called “oscillations.” Thus, once the number of InsP_3Rs that have bound InsP_3 and are thus susceptible to release Ca^{2+} becomes sufficient, their Ca^{2+} -releasing activity becomes both coherent and periodic (12–14).

Given that both a stochastic and deterministic regime can be observed in the same cell for different levels of stimuli, one can intuitively expect that the frontier between the two regimes is not clear-cut and that some “intermediate” behavior can sometimes be observed. In particular, one can wonder to what extent global Ca^{2+} oscillations are really periodic, or if there is a significant random variation in the period during a spike train in a given cell at a fixed concentration of stimulus. Nonlinear time series analysis methods applied to experimental Ca^{2+} traces in hepatocytes suggest that stochasticity is an important factor in the dynamics of intracellular Ca^{2+} oscillations (15). This question can also be raised from the consideration that the number of membrane receptors, ion channels, and Ca^{2+} ions in some membrane organelles in the cell can be very low. Following this examination, a number of modeling studies are built on stochastic simulations of Ca^{2+} dynamics (16–22). These studies have led to interesting conclusions as to the various sensitivities of the different oscillatory regimes to the low numbers of particles or the possible predominance of the stochastic regime in the generation of apparently regular Ca^{2+} oscillations.

In this study, we follow a combined experimental and computational approach to investigate the possible impact of stochasticity on Ca^{2+} oscillations in hepatocytes. Our analysis is based on an estimation of the regularity of Ca^{2+} oscillations in this cell type, in response to stimulation by norepinephrine (Nor). Stochastic simulations of Ca^{2+} oscillations using Gillespie's algorithm are then developed to seek conditions in which one can recover the experimentally measured standard deviations on the period, taking into account realistic con-

Submitted March 20, 2008, and accepted for publication May 7, 2008.

Address reprint requests to G. Dupont, Université Libre de Bruxelles, Faculté des Sciences, Campus Plaine CP231, Boulevard du Triomphe, B-1050 Brussels, Belgium. Tel.: 32-2-650-5794. Fax: 32-2-650-57-67. E-mail: gdupont@ulb.ac.be.

Editor: Ian Parker.

© 2008 by the Biophysical Society
0006-3495/08/09/2193/10 \$2.00

doi: 10.1529/biophysj.108.133777

centrations of Ca^{2+} ions and InsP_3Rs . Comparison between these simulations of the spatially averaged intracellular Ca^{2+} dynamics and experiments in the near vicinity of the bifurcation point provides convincing evidence that hepatocytes display an oscillatory regime strongly affected by internal fluctuations that result from the low number of clusters of InsP_3Rs . The impact of other factors as the InsP_3R isoforms or the possible accompanying InsP_3 oscillations on the regularity of the Ca^{2+} spikes is also addressed.

MATERIALS AND METHODS

Experiments

Materials

Dulbecco's modified Eagle's medium and Williams' medium were from Life Technology (Invitrogen, Cergy-pontoise, France), Collagenase A from Boehringer (Roche Diagnostics, Meylan, France). Other chemicals were purchased from Sigma (Sigma-Genosys, Sigma-Aldrich Chimie, St. Quentin Fallavier, France).

Hepatocyte preparation

Hepatocytes were prepared from fed female Wistar rats by limited collagenase digestion of rat liver, as previously described (23). Experiments were conducted according to the CEE directives for animal experimentation (decree 2001-131; "J.O." 06/02/01). After isolation, rat hepatocytes were maintained (2106 cells/mL) at 4°C in Williams medium E supplemented with 10% fetal calf serum, penicillin (200,000 U/mL), and streptomycin (100 mg/mL). Cell viability, assessed by trypan blue exclusion, remained $>96\%$ for 4–5 h.

HEK293 cell culture

HEK293 cells were cultured in Dulbecco's modified Eagle's medium supplemented with 10% fetal bovine serum, 100 units/mL penicillin, 100 $\mu\text{g/mL}$ streptomycin, and 2 mM glutamine. Cells were grown in an incubator at 37°C with humidified 5% CO_2 and 95% air.

Cellular Ca^{2+} imaging

HEK293 cells grown for 48 h on 35-mm glass cover slips were loaded with 3 μM Fura2-AM at 20°C for 30 min in saline solution containing 20 mM HEPES, 116 mM NaCl, 5.4 mM KCl, 1.8 mM CaCl_2 , 0.8 mM MgCl_2 , 0.96 mM NaH_2PO_4 , 5 mM NaHCO_3 , and 1 g/L glucose (pH 7.4). Cells were then washed twice and kept in the dark at 20°C for at least 20 min. Determination of calcium changes in hepatocytes was as previously described (23). Briefly, hepatocytes were plated onto glass coverslips coated with type I collagen and loaded with 3 μM Fura2-AM in modified Williams' medium, for 40 min (37°C , 5% CO_2). After washing, the coverslips were transferred into a perfusion chamber placed on the stage of a Zeiss inverted microscope (Axiovert 35). Calcium imaging was performed as described previously (23). Fluorescence images were collected by a CCD camera (Princeton Instruments, Trenton, NJ), digitized, and integrated in real time by an image processor (Metafluor, Princeton, NJ).

Computation

The numerical procedure used to simulate Ca^{2+} oscillations is based on stochastic simulations of the transitions among the various states of the InsP_3 -sensitive Ca^{2+} channel. These states and the possible transitions among them are schematized in Fig. 1. This model has been previously used to simulate Ca^{2+} blips and puffs (24). Many other models taking into account

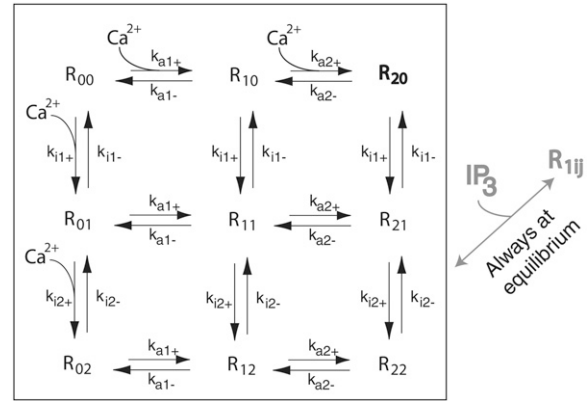


FIGURE 1 Schematic representation of the model used to simulate the dynamics of the $\text{InsP}_3\text{R}/\text{Ca}^{2+}$ channel. The channel exhibits different states, depending on the absence or presence of Ca^{2+} at the binding sites: R_{ij} refers to the state of the channel with i Ca^{2+} ions bound at the activating site and j Ca^{2+} ions bound at the inhibiting site. Binding of InsP_3 is assumed to be always at equilibrium. Cooperativity in Ca^{2+} binding at both sites is accounted for by the fact that $k_{a2+} \gg k_{a1+}$, $k_{a2-} \ll k_{a1-}$, $k_{i2+} \gg k_{i1+}$ and $k_{i2-} \ll k_{i1-}$.

the positive feedback exerted by Ca^{2+} on its own release have been proposed (25). The regulation of the receptor by InsP_3 is not modeled dynamically: InsP_3 binding and unbinding indeed occur on a faster time scale than other processes and can thus be assumed to always be at quasiequilibrium. Thus, the number of open $\text{InsP}_3\text{Rs}/\text{Ca}^{2+}$ channels is given by:

$$R_{20} \frac{[\text{InsP}_3]}{K_D + [\text{InsP}_3]}, \quad (1)$$

where R_{20} represents the number of InsP_3Rs having two Ca^{2+} ions bound at their activation site and no Ca^{2+} ion bound at their inhibitory site (Fig. 1), and K_D the half-saturation constant of InsP_3 for its receptor. Ca^{2+} fluxes across the ER membrane are also modeled stochastically. If v_1 is the total Ca^{2+} flux through the InsP_3Rs when they are all in an open state, the corresponding deterministic evolution equation for cytosolic Ca^{2+} concentration (C) is:

$$\frac{dC}{dt} = \beta[J_{\text{rel}} - J_{\text{serca}}] \quad \text{with} \quad J_{\text{rel}} = v_1 \frac{R_{20}}{R_T} \frac{[\text{InsP}_3]}{K_D + [\text{InsP}_3]} + v_2,$$

$$\text{and} \quad J_{\text{serca}} = v_3 \frac{C^2}{K_3 + C^2}, \quad (2)$$

where β stands for the effective buffering capacity of the cytoplasm and R_T the total number of InsP_3Rs in the cell. Such treatment of buffering relies on the assumptions that cytosolic Ca^{2+} is buffered rapidly and that the fraction of buffered Ca^{2+} remains constant (26). Parameter v_2 represents an unregulated Ca^{2+} leak from the endoplasmic reticulum (ER). Because the concentration of Ca^{2+} in the ER is much higher than that in the cytosol, it is assumed to remain constant. Pumping from the cytosol into the ER is modeled by a Hill function (Hill coefficient equal to 2), with maximal velocity and half-saturation constant represented by v_3 and K_3 , respectively.

We use Gillespie's algorithm (27), which calculates trajectories governed by the chemical master equation and has been abundantly described elsewhere (16,20,28). This method of the Monte-Carlo type associates a probability to each kinetic transition considered in the reaction scheme. This probability depends on the specific stochastic reaction rate and on a combinatorial term that depends on the stoichiometry of the reaction. At each time step, the algorithm randomly determines the reaction that takes place according to its relative probability as well as the time interval to the next reaction step. In the case of the model for Ca^{2+} oscillations, these transitions

are schematized in Table 1, together with the manner by which the numbers of molecules of the different species are updated at each time step. Parameter values (Table 2) are such that, at steady state, the model reproduces the well-known bell-shaped curve for the open probability of the InsP_3R (29,30) as shown in Fig. 2.

RESULTS

Statistical analysis of Ca^{2+} oscillations in hepatocytes

Time series of oscillations of Ca^{2+} -induced fluorescence from hepatocytes stimulated by Nor were analyzed. These data were obtained as explained above (see Materials and Methods). We did not consider traces showing fewer than 10 Ca^{2+} peaks. Typical Ca^{2+} oscillations in hepatocytes stimulated by 0.1 μM and 1 μM Nor are shown in Fig. 3, *A* and *B*, respectively. For each time series, we have independently computed the mean period of Ca^{2+} oscillations and the standard deviation around this mean value. We then pooled the data obtained for cells stimulated by 0.1 μM and 1 μM Nor, respectively. Fig. 4 shows the resulting histograms of the coefficients of variation (CV, i.e., the standard deviation divided by the mean and expressed as a percentage) that have been evaluated. These coefficients largely vary from one cell to another, with an average value of the order of 13% for the lower Nor concentration and 11% for the higher concentra-

tion. The average periods of oscillations are equal to 45.5 ± 5.9 s and 26.0 ± 2.9 s for 0.1 μM and 1 μM Nor, respectively. These values (the average interspike interval and the CV) were very similar for all cell preparations ($n = 9$).

Stochastic simulations of Ca^{2+} oscillations in hepatocytes

In deterministic simulations and for the range of parameters listed in Table 2, sustained oscillations in Ca^{2+} concentration occur for a finite range of InsP_3 concentrations (from 0.09 μM to 5.10 μM). Such simulations adequately describe the real Ca^{2+} dynamics if the number of Ca^{2+} ions and InsP_3Rs are large enough so that internal fluctuations can be neglected. The real number of free Ca^{2+} ions can easily be evaluated from the intracellular concentration and the cytoplasmic volume of a hepatocyte. Thus, assuming a volume of 5×10^{-13} L for the cytoplasm of a hepatocyte (approximated as a sphere whose diameter equals 10 μm), a basal concentration of 100 nM in the cytoplasm corresponds to $\sim 30,000$ Ca^{2+} ions. At the top of a spike, this number is increased by a factor of the order of 10. In the approach proposed by Gillespie (27), a parameter denoted Ω permits the modulation of the number of molecules present in the system. A value of Ω equal to 3×10^5 allows us to get the approximate numbers of free Ca^{2+} ions in our stochastic simulations (Fig. 5). The

TABLE 1 Stochastic model for Ca^{2+} oscillations

| Reaction step | Probability | Changes in particle numbers |
|--|--|---|
| $\text{R}_{00} + \text{C} \rightarrow \text{R}_{10}$ | $k_{a1+} \text{C R}_{00} / \Omega$ | $\text{R}_{00} \rightarrow \text{R}_{00} - 1; \text{R}_{10} \rightarrow \text{R}_{10} + 1; \text{C} \rightarrow \text{C} - 1$ |
| $\text{R}_{10} \rightarrow \text{R}_{00} + \text{C}$ | $k_{a1-} \text{R}_{10}$ | $\text{R}_{10} \rightarrow \text{R}_{10} - 1; \text{R}_{00} \rightarrow \text{R}_{00} + 1; \text{C} \rightarrow \text{C} + 1$ |
| $\text{R}_{10} + \text{C} \rightarrow \text{R}_{20}$ | $k_{a2+} \text{C R}_{10} / \Omega$ | $\text{R}_{10} \rightarrow \text{R}_{10} - 1; \text{R}_{20} \rightarrow \text{R}_{20} + 1; \text{C} \rightarrow \text{C} - 1$ |
| $\text{R}_{20} \rightarrow \text{R}_{10} + \text{C}$ | $k_{a2-} \text{R}_{20}$ | $\text{R}_{20} \rightarrow \text{R}_{20} - 1; \text{R}_{10} \rightarrow \text{R}_{10} + 1; \text{C} \rightarrow \text{C} + 1$ |
| $\text{R}_{01} + \text{C} \rightarrow \text{R}_{11}$ | $k_{a1+} \text{C R}_{01} / \Omega$ | $\text{R}_{01} \rightarrow \text{R}_{01} - 1; \text{R}_{11} \rightarrow \text{R}_{11} + 1; \text{C} \rightarrow \text{C} - 1$ |
| $\text{R}_{11} \rightarrow \text{R}_{01} + \text{C}$ | $k_{a1-} \text{R}_{11}$ | $\text{R}_{11} \rightarrow \text{R}_{11} - 1; \text{R}_{01} \rightarrow \text{R}_{01} + 1; \text{C} \rightarrow \text{C} + 1$ |
| $\text{R}_{11} + \text{C} \rightarrow \text{R}_{21}$ | $k_{a2+} \text{C R}_{11} / \Omega$ | $\text{R}_{11} \rightarrow \text{R}_{11} - 1; \text{R}_{21} \rightarrow \text{R}_{21} + 1; \text{C} \rightarrow \text{C} - 1$ |
| $\text{R}_{21} \rightarrow \text{R}_{11} + \text{C}$ | $k_{a2-} \text{R}_{21}$ | $\text{R}_{21} \rightarrow \text{R}_{21} - 1; \text{R}_{11} \rightarrow \text{R}_{11} + 1; \text{C} \rightarrow \text{C} + 1$ |
| $\text{R}_{02} + \text{C} \rightarrow \text{R}_{12}$ | $k_{a1+} \text{C R}_{02} / \Omega$ | $\text{R}_{02} \rightarrow \text{R}_{02} - 1; \text{R}_{12} \rightarrow \text{R}_{12} + 1; \text{C} \rightarrow \text{C} - 1$ |
| $\text{R}_{12} \rightarrow \text{R}_{02} + \text{C}$ | $k_{a1-} \text{R}_{12}$ | $\text{R}_{12} \rightarrow \text{R}_{12} - 1; \text{R}_{02} \rightarrow \text{R}_{02} + 1; \text{C} \rightarrow \text{C} + 1$ |
| $\text{R}_{12} + \text{C} \rightarrow \text{R}_{22}$ | $k_{a2+} \text{C R}_{12} / \Omega$ | $\text{R}_{12} \rightarrow \text{R}_{12} - 1; \text{R}_{22} \rightarrow \text{R}_{22} + 1; \text{C} \rightarrow \text{C} - 1$ |
| $\text{R}_{22} \rightarrow \text{R}_{12} + \text{C}$ | $k_{a2-} \text{R}_{22}$ | $\text{R}_{22} \rightarrow \text{R}_{22} - 1; \text{R}_{12} \rightarrow \text{R}_{12} + 1; \text{C} \rightarrow \text{C} + 1$ |
| $\text{R}_{00} + \text{C} \rightarrow \text{R}_{01}$ | $k_{i1+} \text{C R}_{00} / \Omega$ | $\text{R}_{00} \rightarrow \text{R}_{00} - 1; \text{R}_{01} \rightarrow \text{R}_{01} + 1; \text{C} \rightarrow \text{C} - 1$ |
| $\text{R}_{01} \rightarrow \text{R}_{00} + \text{C}$ | $k_{i1-} \text{R}_{01}$ | $\text{R}_{01} \rightarrow \text{R}_{01} - 1; \text{R}_{00} \rightarrow \text{R}_{00} + 1; \text{C} \rightarrow \text{C} + 1$ |
| $\text{R}_{01} + \text{C} \rightarrow \text{R}_{02}$ | $k_{i2+} \text{C R}_{01} / \Omega$ | $\text{R}_{01} \rightarrow \text{R}_{01} - 1; \text{R}_{02} \rightarrow \text{R}_{02} + 1; \text{C} \rightarrow \text{C} - 1$ |
| $\text{R}_{02} \rightarrow \text{R}_{01} + \text{C}$ | $k_{i2-} \text{R}_{02}$ | $\text{R}_{02} \rightarrow \text{R}_{02} - 1; \text{R}_{01} \rightarrow \text{R}_{01} + 1; \text{C} \rightarrow \text{C} + 1$ |
| $\text{R}_{10} + \text{C} \rightarrow \text{R}_{11}$ | $k_{i1+} \text{C R}_{10} / \Omega$ | $\text{R}_{10} \rightarrow \text{R}_{10} - 1; \text{R}_{11} \rightarrow \text{R}_{11} + 1; \text{C} \rightarrow \text{C} - 1$ |
| $\text{R}_{11} \rightarrow \text{R}_{10} + \text{C}$ | $k_{i1-} \text{R}_{11}$ | $\text{R}_{11} \rightarrow \text{R}_{11} - 1; \text{R}_{10} \rightarrow \text{R}_{10} + 1; \text{C} \rightarrow \text{C} + 1$ |
| $\text{R}_{11} + \text{C} \rightarrow \text{R}_{12}$ | $k_{i2+} \text{C R}_{11} / \Omega$ | $\text{R}_{11} \rightarrow \text{R}_{11} - 1; \text{R}_{12} \rightarrow \text{R}_{12} + 1; \text{C} \rightarrow \text{C} - 1$ |
| $\text{R}_{12} \rightarrow \text{R}_{11} + \text{C}$ | $k_{i2-} \text{R}_{12}$ | $\text{R}_{12} \rightarrow \text{R}_{12} - 1; \text{R}_{11} \rightarrow \text{R}_{11} + 1; \text{C} \rightarrow \text{C} + 1$ |
| $\text{R}_{20} + \text{C} \rightarrow \text{R}_{21}$ | $k_{i1+} \text{C R}_{20} / \Omega$ | $\text{R}_{20} \rightarrow \text{R}_{20} - 1; \text{R}_{21} \rightarrow \text{R}_{21} + 1; \text{C} \rightarrow \text{C} - 1$ |
| $\text{R}_{21} \rightarrow \text{R}_{20} + \text{C}$ | $k_{i1-} \text{R}_{21}$ | $\text{R}_{21} \rightarrow \text{R}_{21} - 1; \text{R}_{20} \rightarrow \text{R}_{20} + 1; \text{C} \rightarrow \text{C} + 1$ |
| $\text{R}_{21} + \text{C} \rightarrow \text{R}_{22}$ | $k_{i2+} \text{C R}_{21} / \Omega$ | $\text{R}_{21} \rightarrow \text{R}_{21} - 1; \text{R}_{22} \rightarrow \text{R}_{22} + 1; \text{C} \rightarrow \text{C} - 1$ |
| $\text{R}_{22} \rightarrow \text{R}_{21} + \text{C}$ | $k_{i2-} \text{R}_{22}$ | $\text{R}_{22} \rightarrow \text{R}_{22} - 1; \text{R}_{21} \rightarrow \text{R}_{21} + 1; \text{C} \rightarrow \text{C} + 1$ |
| $\text{C}_{\text{ER}} \xrightarrow{\text{InsP}_3 \text{R}} \text{C}$ | $v_1 \frac{R_{20}}{R_T K_D + [\text{InsP}_3]}$ | $\text{C} \rightarrow \text{C} + 1$ |
| $\text{C}_{\text{ER}} \xrightarrow{\text{leak}} \text{C}$ | $v_2 \Omega$ | $\text{C} \rightarrow \text{C} + 1$ |
| $\text{C} \rightarrow \text{C}_{\text{ER}}$ | $v_3 \frac{\text{C}^2}{K_3 + \text{C}^2} \Omega$ | $\text{C} \rightarrow \text{C} - 1$ |

The first column lists the sequence of reactions. The probability that each reaction will occur within an infinitesimal time interval is given in the second column. The last column indicates the changes in the number of molecules/ions taking part in the different reactions.

TABLE 2 Parameter values used in Gillespie's simulations of Ca^{2+} oscillations

| Parameter | Description | Value |
|-----------|--|---|
| k_{a1+} | Ca^{2+} binding to the first activating site of the InsP_3R | $350 \mu\text{M}^{-1}\text{s}^{-1}$ |
| k_{a2+} | Ca^{2+} binding to the second activating site of the InsP_3R | $20,000 \mu\text{M}^{-1}\text{s}^{-1}$ |
| k_{a1-} | Ca^{2+} dissociation from the first activating site of the InsP_3R | 3000 s^{-1} |
| k_{a2-} | Ca^{2+} dissociation from the second activating site of the InsP_3R | 30 s^{-1} |
| k_{i1+} | Ca^{2+} binding to the first inhibiting site of the InsP_3R | $0.5 (0.2) \mu\text{M}^{-1}\text{s}^{-1}$ |
| k_{i2+} | Ca^{2+} binding to the second inhibiting site of the InsP_3R | $100 (20) \mu\text{M}^{-1}\text{s}^{-1}$ |
| k_{i1-} | Ca^{2+} dissociation from the first inhibiting site of the InsP_3R | 25 s^{-1} |
| k_{i2-} | Ca^{2+} dissociation from the second inhibiting site of the InsP_3R | 0.2 s^{-1} |
| β | Ca^{2+} buffering capacity of the cytoplasm | 0.05 |
| K_D | Half-saturation constant of InsP_3 for its receptor | $0.35 \mu\text{M}$ |
| v_1 | Maximal rate of Ca^{2+} release through the InsP_3R | $600 \mu\text{M}^{-1}\text{s}^{-1}$ |
| v_2 | Ca^{2+} leak from the ER | $2 \mu\text{M}^{-1}\text{s}^{-1}$ |
| v_3 | Maximal rate of Ca^{2+} pumping into the ER | $100 \mu\text{M}^{-1}\text{s}^{-1}$ |
| K_3 | Half saturation constant of Ca^{2+} pumping into the ER | $0.1 \mu\text{M}$ |
| R_T | Total number of clusters of InsP_3Rs considered in the simulations | 9–5400 |
| Ω | Parameter of Gillespie's algorithm allowing to modulate the number of Ca^{2+} ions | $3 \cdot 10^5$ |

As described in the Materials and Methods section and in Table 1. Values in parentheses refer to the modeling of the other isoform of the InsP_3R shown in Fig. 8. The value of parameter R_T is given in the legends for each figure.

number of InsP_3Rs is more difficult to evaluate. In guinea pig hepatocytes, the number of monomeric InsP_3Rs has been estimated to be $\sim 190 \text{ fmol/mg protein}$ (31), which amounts to a density of tetrameric receptors equal to $1.31 \times 10^{16}/\text{L}$. This density is ~ 100 times higher than that in *Xenopus* oocytes and 200 times lower than is found in Purkinje cells of the cerebellum (32). In the volume of a typical hepatocyte, the density reported by Spät et al. (31) corresponds to ~ 6000 InsP_3Rs . This number will determine the value of R_T (total number of InsP_3Rs or InsP_3R clusters) that has to be introduced in the simulations.

Typical oscillations obtained by stochastic simulations of the model are shown in Fig. 5 A. Taking into account a number of InsP_3Rs in the range of what has been estimated above (5400 receptors), these oscillations are very regular. In these conditions, indeed, the CV of the period is equal to 2.4%, a value that is smaller than any value measured experimentally. Even for other values for the kinetic parameters

used in the simulations, the CV never exceeds 5%. Based on previous studies suggesting that InsP_3Rs are clustered in different cell types (24,33), we then supposed that the channels are arranged in groups of 25. In the simulations, a cluster of n receptors is modeled as one channel with an n -fold larger conductance than an isolated receptor; indeed, if the receptors inside the cluster are assumed to be in close contact, the Ca^{2+} concentration in their vicinity is the same, and, thus, in first approximation, they all open and close simultaneously. Fig. 5 B clearly shows that the regularity greatly decreases in these conditions; the CV on the period is then equal to 13.9%, which is of the order of experimental estimations (see also Fig. 3 A). Because the number of clusters in this case is rather low ($5400/25 = 216$), the variability on the period greatly differs with the number of clusters in this range. This is shown in Fig. 6, where the total conductance of all InsP_3Rs is kept constant. For large numbers of small groups of InsP_3Rs (with a limit situation of 5400 single channels), the CV becomes very small as one recovers the nearly deterministic case shown in Fig. 5 A (see also Fig. 6, point c). Interestingly, the CV does not vanish, even if one increases the number of clusters up to a value that corresponds to an unrealistically high number of InsP_3Rs (not shown). The remaining $\sim 1.5\%$ of variability can be ascribed to the relatively low number of Ca^{2+} ions. At the other extremity, i.e., for a very small number of large clusters, the oscillations become unrealistically irregular (Fig. 6, point a inset).

As expected, variability also decreases with the concentration of InsP_3 . A decrease in InsP_3 concentration indeed corresponds to a lower number of channels taking an active part in Ca^{2+} release. Below the deterministic oscillatory regime, subthreshold InsP_3 concentrations lead to widely spaced, very irregular spikes; this is visible in the first part of Fig. 7 A, where the level of InsP_3 is just below the bifurcation point delimiting the oscillatory domain and would thus correspond to a stable steady state in the deterministic regime. However, because this state is excitable, when fluctuations are allowed to occur, they can sometimes pass the threshold for excitability and generate a whole Ca^{2+} spike. This autonomous stochastic resonance phenomenon, which can be obtained only with a small number of Ca^{2+} -releasing channels, has also been observed in other models for Ca^{2+} oscillations (20,33,34). Such noise-induced Ca^{2+} oscillations are characterized by large standard deviations on the mean interspike interval (35% in the case of Fig. 7 A). To compare, just on the other side of the bifurcation point ($[\text{InsP}_3] = 0.095 \mu\text{M}$), oscillations are much more regular (17% in the case of the second part of Fig. 7 A). Such a steep change in the regularity of Ca^{2+} oscillations can sometimes be observed in hepatocytes, when the level of Nor is finely adjusted at the border of the oscillatory domain (Fig. 7 B). A subthreshold concentration of Nor ($0.03 \mu\text{M}$) induces noisy and irregular Ca^{2+} oscillations (CV = 31%). A slight increase of the Nor concentration ($0.05 \mu\text{M}$) then provokes a significant increase in the regularity of oscillations (CV = 12%), which becomes

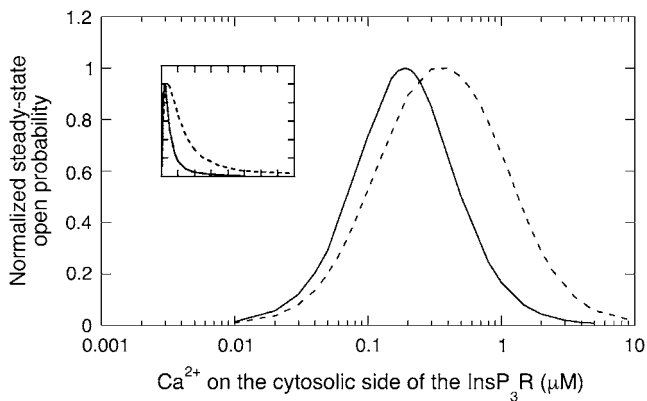


FIGURE 2 Stationary open probability of the InsP_3R obtained by solving the evolution equations of the model schematized in Fig. 1 at steady state. The two curves correspond to different isoforms of the receptor. The solid line is compatible with a form of the receptor that is very sensitive to Ca^{2+} changes (possibly type 2), and the dashed line would correspond to a wider bell-shaped curve, which is slightly shifted to the right (possibly type 1). The inset corresponds to the same curves shown in linear scale. The receptor whose behavior is illustrated by the solid line has been used for all figures except for Fig. 8 where parameter values corresponding to the dashed line have been used. Parameter values are those listed in Table 2 with $[\text{InsP}_3] = 0.1 \mu\text{M}$, with the dashed line corresponding to the values indicated in parentheses. Both curves are normalized with respect to their maxima, i.e., 0.19 for the solid line and 0.79 for the dashed line. See Dupont and Combettes (39) for more details about the modeling of the InsP_3R isoforms.

qualitatively similar to the repetitive spikes observed in the whole oscillatory domain (Fig. 4). The results shown in Fig. 7 reveal two important dynamical characteristics of Ca^{2+} oscillations in hepatocytes: first, that the number of clusters of InsP_3Rs is low, allowing the existence of noise-induced Ca^{2+} oscillations, and, second, that for most stimulation levels, oscillations occur in a deterministically oscillatory regime, where the CV is much smaller than that for noise-induced Ca^{2+} oscillations.

Other factors affecting the regularity of Ca^{2+} oscillations

Observations of Ca^{2+} oscillations in different cell types suggest that their regularity varies among cell types (35). Many factors can be involved in this effect, such as the size of the cell and the receptor density. The respective amounts of the InsP_3R isoforms could also play a role in this respect. Three isoforms of this channel, differing in their regulatory properties by Ca^{2+} and InsP_3 , have indeed been identified. These are coexpressed within cells, but their respective levels of expression are largely tissue- and development-specific (36). The amounts of each isoform of a given subtype have been modified by genetic manipulations in DT40, HeLa, and COS-7 cells, leading to the idea that there is a close correlation between the types of InsP_3Rs present in a cell and the existence, characteristics, and regularity of Ca^{2+} oscillations (37,38).

In a previous study based on a deterministic approach (39), we have shown that slight modifications in the regulatory properties of the InsP_3Rs can lead to significantly different oscillatory properties when their respective densities are varied. Here, we perform stochastic simulations to test whether the robustness of Ca^{2+} oscillations can also be affected by the receptor subtype. Thus, we change the parameter values characterizing the InsP_3R dynamics to change the shape of the bell-shaped curve showing the channel-opening probability (Fig. 2). Qualitatively, the changes performed correspond to a channel that is less sensitive to Ca^{2+} changes (wider bell-shaped curve) and that is activated by slightly higher Ca^{2+} concentrations. In reality, this subtype is associated with a dependence of the level of Ca^{2+} corresponding to the highest opening probability on the InsP_3 level (shift of the bell-shaped curve with the InsP_3 concentration), but because this simulations are performed with a constant InsP_3 concentration, it is only reflected by different kinetic parameters leading to a wider bell-shaped curve (rate of Ca^{2+} binding to and unbinding from the inhibitory binding site, see Table 2).

At low stimulation levels, Ca^{2+} oscillations generated by the InsP_3R characterized by the wider bell-shaped curve show approximately the same CV as those obtained before (Fig. 8). Interestingly, the CV rapidly increases with InsP_3 concentration. Intuitively, one can understand that: because Ca^{2+} -induced inhibition is less efficient (wider bell-shaped

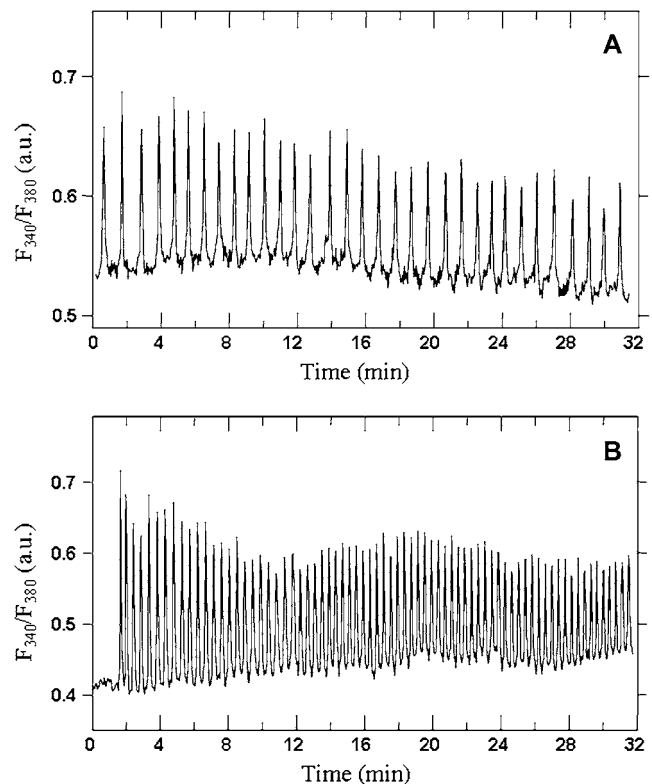


FIGURE 3 Typical Ca^{2+} oscillations in Nor-stimulated hepatocytes. The concentration of Nor is $0.1 \mu\text{M}$ (A) or $1 \mu\text{M}$ (B).

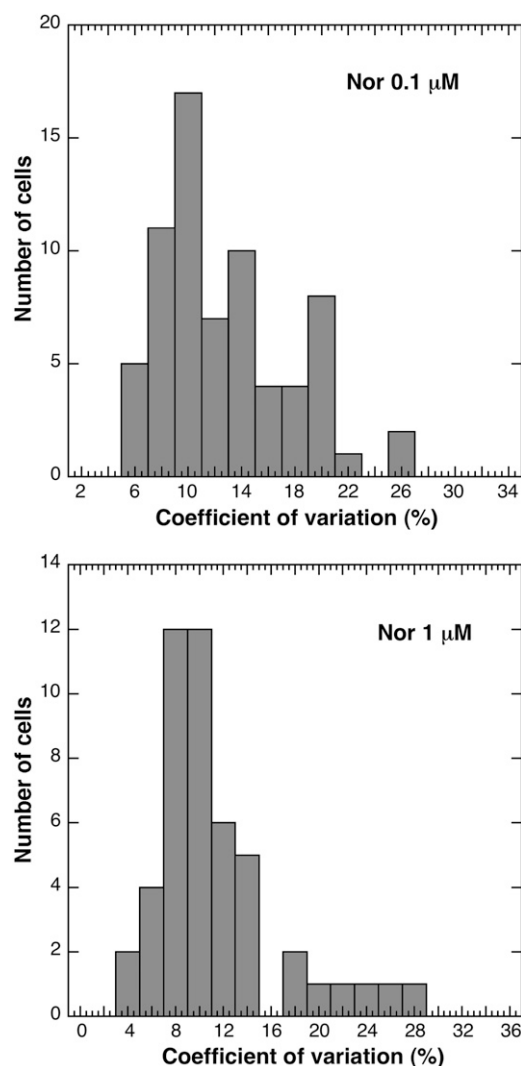


FIGURE 4 Histograms of the CVs calculated from experimental time series of Ca^{2+} oscillations in hepatocytes stimulated by Nor. The upper panel synthesizes the measurements performed in 68 cells, all stimulated by $0.1 \mu\text{M}$ Nor. The average CV equals 13%, and the average period 45.5 s. For the lower panel ($n = 47$), other cells were stimulated by $1 \mu\text{M}$ Nor. The average CV and period equal 11% and 26.0 s, respectively. For both panels, all cells considered displayed more than 10 Ca^{2+} spikes whose maximum was always larger than the average fluorescence.

curve), these InsP_3R can sometimes remain open longer, leading to prolonged Ca^{2+} peaks like those shown in the inset of Fig. 8. This in turn induces a higher variability of the period. From a different point of view, because a widening of the bell-shaped curve is associated with a decrease in the range of InsP_3 concentrations leading to oscillations, fluctuations occasionally push the system out of the oscillatory regime, thus leading to an incident increase of the spike width and thereby of the interspike interval. Interestingly, this also induces an increase of the CV with the level of InsP_3 , whereas the opposite was obtained for the other parameter values as well as observed in hepatocytes.

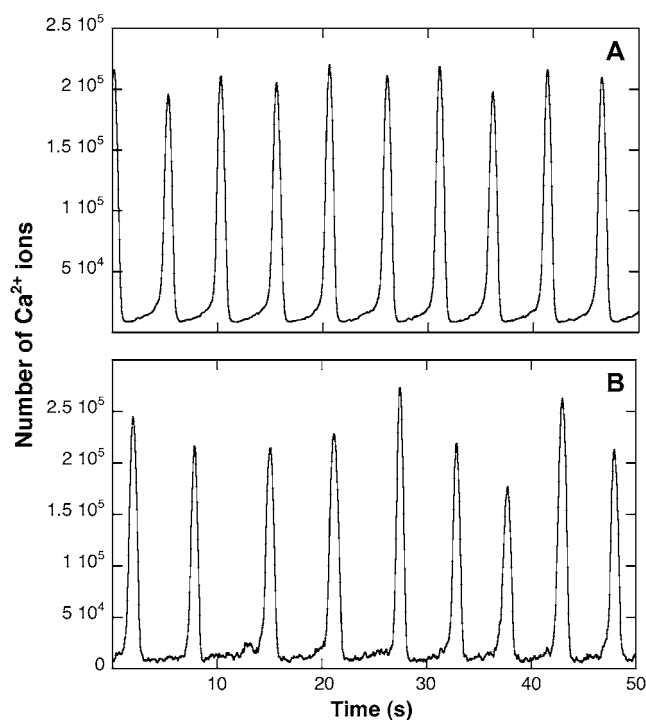


FIGURE 5 Gillespie's simulations of Ca^{2+} oscillations. (A) All InsP_3R s (5400) are considered to be independently regulated by Ca^{2+} . (B) The InsP_3R s are assumed to be clustered in groups of 25 channels; thus, $R_T = 216$. Each group of 25 channels is modeled, in first approximation, as one "megachannel" because it is assumed that all channels open simultaneously and subsequently become inhibited at the same time. The conductance of this megachannel is 25 times the conductance of a single InsP_3R . For both panels, reactions and parameters are given in Tables 1 and 2. $[\text{InsP}_3] = 0.2 \mu\text{M}$.

In a hypothetical way, one can assume that the wider bell-shaped curve is approaching the type 1 InsP_3R , whereas the original parameters would qualitatively more closely correspond to the $\text{InsP}_3\text{R}2$, which is predominantly expressed in hepatocytes. In this framework, indirect confirmation of these higher values for the CV when widening the bell-shaped curve is given by the analysis of Ca^{2+} oscillations in human embryonic kidney (HEK) cells, a cell line that expresses only type 1 and type 3 receptors. An analysis of time series of Ca^{2+} oscillations in HEK cells stimulated either by ATP or carbachol indeed indicates an average CV equal to 31% ($n = 30$). An example of such a time series is given in Fig. 9, where a broadening of the spikes similar to what is seen in the simulations can be observed. A similar value for the CV has been estimated from the analysis of the interspike intervals in HEK cells stimulated with carbachol (35).

Finally, we have used our stochastic model to investigate the effect of potential InsP_3 variations accompanying Ca^{2+} oscillations on the regularity of the interspike intervals. Observations performed in epithelial (40) or Chinese hamster ovary (41) cells indeed suggest that Ca^{2+} and InsP_3 could oscillate in synchrony. It is plausible that both oscillatory mechanisms (InsP_3 -driven or not) could coexist in different

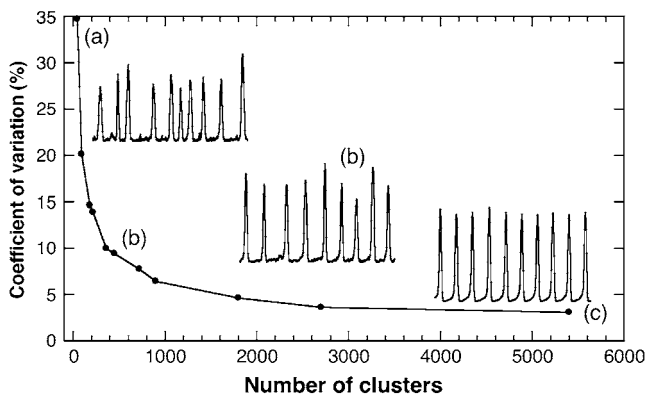


FIGURE 6 Relation between the CV and the number of clusters, R_T , in the stochastic model for Ca^{2+} oscillations. The total Ca^{2+} flux through all the InsP_3 Rs is assumed to remain constant. The insets show oscillations on a 100-s period of time, obtained with 45 (a), 216 (b), or 5400 (c) clusters. All the simulations are performed with reactions and parameters given in Tables 1 and 2, with $[\text{InsP}_3] = 0.2 \mu\text{M}$.

cell types (42). InsP_3 oscillations can result from regulation by Ca^{2+} of either InsP_3 synthesis or InsP_3 degradation; PLC, the enzyme responsible for InsP_3 synthesis, indeed requires Ca^{2+} for its activity, and, for some isoforms, stimulation of PLC activity by Ca^{2+} occurs in the same concentration range as Ca^{2+} oscillations. Also, InsP_3 transformation by the InsP_3 3-kinase is activated by the Ca^{2+} -calmodulin complex (43). Although this regulation is thought to play a minor role in the existence and characteristics of Ca^{2+} oscillations in hepatocytes (23), one might expect that it could lead to a stabilization of the period of oscillations.

We have thus included additional steps in Gillespie's algorithm to model InsP_3 synthesis and degradation. The kinetic expressions used are of the Michaelis type (see legend to Fig. 10). The number of InsP_3 molecules (of the order of 10^5) was chosen to realistically model an InsP_3 concentration of the order of $1 \mu\text{M}$. When Ca^{2+} stimulates InsP_3 synthesis, we found no significant effect of InsP_3 dynamics on the robustness of Ca^{2+} oscillations (Fig. 10): the CV is in the range 10–15% in the whole oscillatory domain. Other simulations where InsP_3 oscillations are provoked by the Ca^{2+} -induced activation of InsP_3 transformation into InsP_4 lead to the same conclusion. As in the simulations shown above, most internal fluctuations are indeed linked to the species that is present in the lowest amount, i.e., the number of clusters of InsP_3 Rs.

DISCUSSION

In this study, we have shown that Ca^{2+} spikes in hepatocytes are intrinsically irregular, as the spikes are paced with a precision that does not exceed 85%. Stochastic simulations incorporating realistic numbers of Ca^{2+} ions and InsP_3 Rs argue that this irregularity can be ascribed to the gathering of InsP_3 Rs in groups of a few tens of channels. The concept of clustering of Ca^{2+} channels is well known to be necessary to

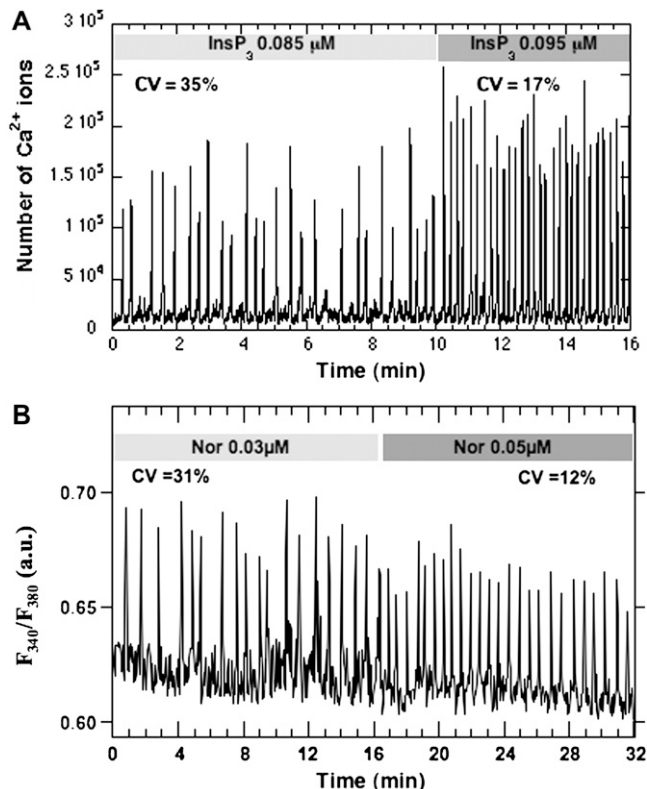


FIGURE 7 Transition from noise-induced Ca^{2+} oscillations to deterministic Ca^{2+} oscillations in hepatocytes. (A) The results of stochastic simulations at an InsP_3 concentration just below the bifurcation point for 10 min. The level of InsP_3 is then instantaneously increased by $0.01 \mu\text{M}$, which provokes the entry in the deterministic oscillatory regime. This change of dynamic regime is accompanied by a large decrease of the CV. (B) An experimental trace of fluorescence obtained in a hepatocyte at two very low concentrations of Nor, which presumably correspond to the passage through the bifurcation point for this particular cell. Such a behavior is rarely observed (fewer than 10% of the cells responding to this low concentration of Nor).

explain the characteristics of smaller-scale Ca^{2+} increases known as “ Ca^{2+} puffs” (17,24,33). This analysis indicates that such a clustering is also necessary to account for the intrinsic irregularity of the repetitive, global Ca^{2+} spikes. Interestingly, it has also been shown that Ca^{2+} signaling capability of the cell is modified with the distribution of the Ca^{2+} release channels; channel clustering can indeed enhance the cell's capability to generate a large response to a weak InsP_3 signal (44). Taken together, this study and the results obtained by Shuai and Jung (44) indicate that the distribution of InsP_3 Rs in clusters is a compromise between optimizing the sensitivity of the cell to weak stimuli and ensuring robust oscillations. Given the important role played by internal fluctuations at the low number of clusters predicted by the oscillations (~ 200), noise-induced Ca^{2+} oscillations sometimes take place in hepatocytes at subthreshold concentrations of Nor. In agreement with the limited InsP_3 range in which such noisy repetitive spiking can be observed in the simulations, this behavior is in fact rarely observed in exper-

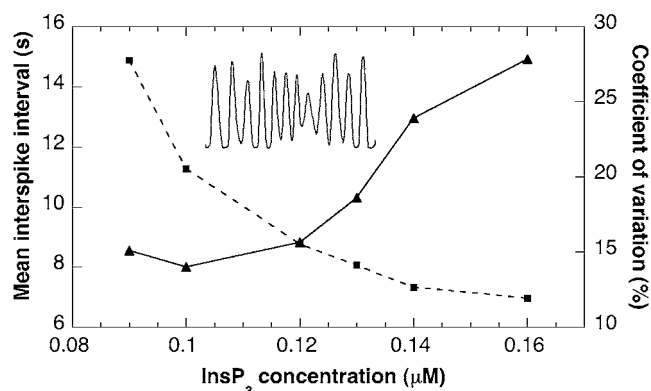


FIGURE 8 Effect of changing the isoform of the InsP_3R on the robustness of Ca^{2+} oscillations. Shown are the mean interspike interval (dashed line) and CV (solid line) obtained by Gillespie's simulations of the model detailed in Table 1, with parameter values shown in Table 2, considering the values indicated in parentheses. As shown by the dashed curve of Fig. 2, these parameters correspond to an InsP_3R isoform that is less sensitive to Ca^{2+} changes. The dependence of the rate of inhibition of the InsP_3R of type 1 on the level of InsP_3 is not considered in the simulations, as it does not influence the robustness of oscillations at constant InsP_3 concentration. The inset shows typical Ca^{2+} oscillations obtained in the simulations. For the inset, $[\text{InsP}_3] = 0.12 \mu\text{M}$, and the mean interspike interval equals 8.8 s; a 100-s simulation is shown.

iments. In other cell types where the density of clusters is larger, such noise-induced Ca^{2+} oscillations are not expected to occur, as the impact of internal fluctuations would be much reduced in this case.

The present results also suggest that for most stimulation levels, experimentally observed Ca^{2+} oscillations in hepatocytes correspond to an oscillatory regime; the steep increase in the CV shown in Fig. 7 indeed corresponds to the passage from an excitable to an oscillatory regime. Studies in other cell types have, however, led to the opposite conclusion (17,19). Instead, Ca^{2+} oscillations are there viewed as a sequence of random spikes (35). This dissent may find its origin in the fact that the oscillations reported in the latter study are

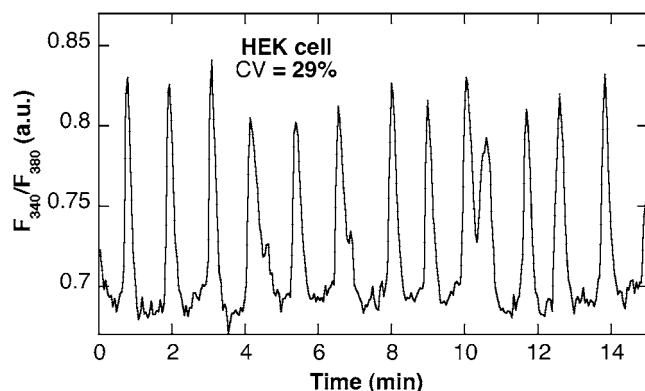


FIGURE 9 Typical oscillations in cytosolic Ca^{2+} in HEK cells stimulated by carbachol. The indicated value of the CV has been established on a total of 54 peaks (representing 55 min of monitoring), among which only 12 are shown here. This value is close to the average value of 31% obtained for 30 cells.

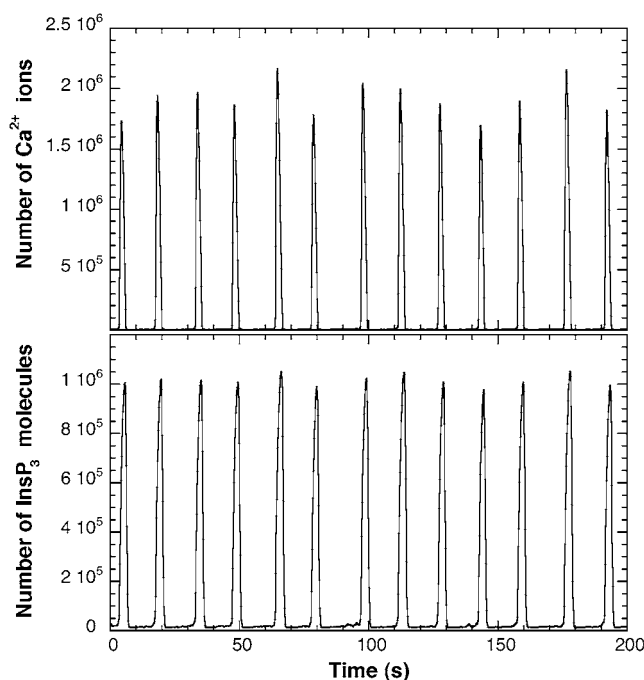


FIGURE 10 Gillespie's simulations of Ca^{2+} oscillations when including InsP_3 oscillations resulting from the positive feedback exerted by Ca^{2+} on PLC activity. Transition rates and parameters are as in Fig. 5, with additional steps corresponding to the stochastic version of the following evolution equation: $d([\text{InsP}_3])/dt = \gamma V_{\text{PLC}}(C/(K_A + C)) - V_d([\text{InsP}_3]/(K_d + [\text{InsP}_3])) - k_{\text{NS}}[\text{InsP}_3]$ with $V_{\text{PLC}} = 100 \mu\text{Ms}^{-1}$; $K_A = 0.3 \mu\text{M}$; $V_d = 5 \mu\text{Ms}^{-1}$; $K_d = 0.6 \mu\text{M}$; $k_{\text{NS}} = 0.5 \text{ s}^{-1}$, and $\gamma = 0.07$. For these parameter values, the CV equals 13.6%.

in most cases spontaneous (i.e., not induced by the application of any hormone); these noisy oscillations may thus rely on another type of dynamics (45). It is, on the other hand, meaningful that different cell types use different ways to display repetitive Ca^{2+} spiking because of structural disparities. In the simulations of Ca^{2+} waves in *Xenopus* oocytes that have suggested a stochastic nature to Ca^{2+} oscillations (17), the so-called "focal sites" made of a group of nearby clusters are responsible for the nucleation of the wave. In this framework, an entire hepatocyte can be viewed as a large focal site, as the mean average distance between clusters is of the order of $1 \mu\text{m}$ (estimated on the basis of ~ 200 clusters). In this respect, it is interesting to mention that puffs have never been reported in hepatocytes. Although one cannot exclude that their observation is in fact limited by technical considerations, this may suggest that the cluster arrangement is such that the firing of any of them will automatically induce a global cytoplasmic Ca^{2+} increase. Other cell-to-cell differences in the regularity of the spikes can be ascribed to the different populations of InsP_3Rs isoforms, which are known to characterize the various cell types (36). Our results indeed suggest that oscillations relying on the type 2 InsP_3R will be particularly robust, which qualitatively fits with the experimental observations performed by Miyakawa et al. (37) in DT40 B cells and by Morel et al. (46) in myocytes.

The period of the simulated Ca^{2+} oscillations presented here is always shorter than in the experiments. This drawback may probably be avoided by taking into account other regulatory processes such as Ca^{2+} exchange with the extracellular medium (47), Ca^{2+} handling by mitochondria (48), the detailed kinetics of the hormonal receptor (18), local luminal Ca^{2+} depletion (49), or a dynamic modeling of buffering (50,51). As shown in previous studies (18), the consideration of this latter factor would slightly decrease the fluctuations in free Ca^{2+} . Although we are aware of the fact that the model is simplified with respect to all these additional controls, our present hypothesis is that such processes would not affect our conclusions as to the robustness of the oscillations, which mainly depends on the number of clusters of InsP_3Rs . In the same manner, we have neglected spatial aspects in the simulations, which are necessary to account for wave propagation. Incorporation of Ca^{2+} diffusion in stochastic modeling is very time-consuming. In most cases, simplifying hypotheses have been introduced (17,49). Another consequence of neglecting spatial aspects is that our representation of clusters where all $\text{InsP}_3\text{Rs}/\text{Ca}^{2+}$ channels open and close together is also oversimplified. More realistic descriptions of clusters can be found elsewhere (17,19,21,24,33,49). We plan to extend this work to incorporate Ca^{2+} diffusion into Gillespie's algorithm, as has been done for the minimal Ca^{2+} -induced Ca^{2+} release model (16).

Because, in vivo, hepatocytes are connected and coupled through gap junctions and display synchronized Ca^{2+} spikes (52), incorporation of Ca^{2+} diffusion will also make it possible to study the effect of intercellular coupling on the robustness of Ca^{2+} oscillations in hepatocytes. The importance of stochastic effects in modeling Ca^{2+} oscillations in connected hepatocytes has already been assessed (53). Of particular interest is the conclusion reached by these authors that fluctuations in intracellular InsP_3 and Ca^{2+} levels decrease the threshold level of gap junction permeability necessary to coordinate Ca^{2+} spiking between adjacent cells. In vivo, an additional level of complexity arises from the fact that the hormonal stimulus does not remain strictly constant and, in some instances, even follows an oscillatory pattern (11,54). Thus, as is nowadays largely emphasized for genetic systems (28,55), molecular noise appears to be an important component of the oscillatory Ca^{2+} dynamics, which has to be considered for a detailed elucidation of this widespread signaling pathway.

We thank Didier Gonze and Stéphane Swillens for very fruitful discussions. G.D. acknowledges support from the Fonds de la Recherche Scientifique Médicale (grant No. 3.4636.04), the European Union through the Network of Excellence BioSim (Contract No. LSHB-CT-2004-005137), and the Belgian Program on Interuniversity Attraction Poles (P6/25-BIOMAGNET). L.C. acknowledges support from Agence Nationale de la Recherche (RPV07094LSA) and Programme National de la Recherche in Hepatogastroenterology. This work was supported by a program of the Institut National de la Santé et de la Recherche Médicale/Communauté Française de Belgique. G.D. is Maître de Recherche at the Belgian Fonds National de

la Recherche Scientifique. A.A. is supported by the Ministère de l'éducation nationale, de la recherche et de la technologie.

REFERENCES

- Berridge, M. J. 1993. Elementary and global aspects of calcium signalling. *J. Physiol.* 499:291–306.
- Spitzer, N., N. Lautermilch, R. Smith, and T. Gomez. 2000. Coding of neuronal differentiation by calcium transients. *Bioessays*. 22:811–817.
- Moraru, I., and L. Loew. 2005. Intracellular signalling: spatial and temporal control. *Physiology (Bethesda)*. 20:169–179.
- Dupont, G., L. Combettes, and L. Leybaert. 2007. Calcium dynamics: spatio-temporal organization from the subcellular to the organ level. *Int. Rev. Cytol.* 261:193–245.
- Swann, K., and J. P. Ozil. 1994. Dynamics of the calcium signal that triggers mammalian egg activation. *Int. Rev. Cytol.* 152:183–222.
- Bers, D., and T. Guo. 2005. Calcium signaling in cardiac ventricular myocytes. *Ann. N. Y. Acad. Sci.* 1047:86–98.
- Leybaert, L., K. Paemeleire, A. Strahonja, and M. Sanderson. 1998. Inositol-trisphosphate-dependent intercellular calcium signalling in and between astrocytes and endothelial cells. *Glia*. 24:398–407.
- Love, J., A. Dodd, and A. Webb. 2004. Circadian and diurnal calcium oscillations encode photoperiodic information in *Arabidopsis*. *Plant Cell*. 16:956–966.
- De Koninck, P., and H. Schulman. 1998. Sensitivity of CaM kinase II to the frequency of Ca^{2+} oscillations. *Science*. 279:227–230.
- Larsen, A., L. F. Olsen, and U. Kummer. 2004. On the encoding and decoding of calcium signals in hepatocytes. *Biophys. Chem.* 107:83–99.
- Goldbeter, A. 1996. *Biochemical Oscillations and Cellular Rhythms*. Cambridge: Cambridge University Press.
- Bootman, M., E. Niggli, M. J. Berridge, and P. Lipp. 1997. Imaging the hierarchical Ca^{2+} signalling system in HeLa cells. *J. Physiol.* 482:533–553.
- Marchant, J., and I. Parker. 2001. Role of elementary Ca^{2+} puffs in generating repetitive Ca^{2+} oscillations. *EMBO J.* 20:65–76.
- Sun, X.-P., N. Callamaras, J. Marchant, and I. Parker. 1998. A continuum of InsP_3 -mediated elementary Ca^{2+} signalling events in *Xenopus* oocytes. *J. Physiol.* 509:67–80.
- Perc, M., A. Green, C. J. Dixon, and M. Marhl. 2008. Establishing the stochastic nature of intracellular calcium oscillations from experimental data. *Biophys. Chem.* 132:33–38.
- Kraus, M., B. Wolf, and B. Wolf. 1996. Crosstalk between cellular morphology and calcium oscillation patterns. *Cell Calcium*. 19:461–472.
- Falcke, M. 2004. Reading the patterns in living cells—the physics of Ca^{2+} signaling. *Adv. Phys.* 53:255–440.
- Kummer, U., B. Krajnc, J. Pahle, A. Green, J. Dixon, and M. Marhl. 2005. Transition from stochastic to deterministic behavior in calcium oscillations. *Biophys. J.* 89:1603–1611.
- Keener, J. 2006. Stochastic calcium oscillations. *Math. Med. Biol.* 23:1–25.
- Zhu, C., Y. Jia, Q. Liu, L. Yang, and X. Zhan. 2006. A mesoscopic stochastic mechanism of cytosolic Ca^{2+} oscillations. *Biophys. Chem.* 125:201–212.
- Shuai, J., J. Pearson, J. Foskett, D. Mak, and I. Parker. 2007. A kinetic model of single and clustered InsP_3 receptors in the absence of Ca^{2+} feedback. *Biophys. J.* 93:1151–1162.
- Williams, G., E. Molinelli, and G. Smith. 2008. Modeling local and global intracellular calcium responses mediated by diffusely distributed inositol 1,4,5-trisphosphate receptors. *J. Theor. Biol.* 253:170–188.
- Dupont, G., O. Koukoui, C. Clair, C. Erneux, S. Swillens, and L. Combettes. 2003. Ca^{2+} oscillations in hepatocytes do not require the modulation of InsP_3 3-kinase activity by Ca^{2+} . *FEBS Lett.* 534:101–105.

24. Swillens, S., G. Dupont, L. Combettes, and P. Champeil. 1999. From calcium blips to calcium puffs: theoretical analysis of the requirements for interchannel communication. *Proc. Natl. Acad. Sci. USA*. 96: 13750–13755.
25. Schuster S., M. Marhl, and T. Höfer. 2002. Modelling of simple and complex calcium oscillations. From single-cell responses to intercellular signalling. *Eur. J. Biochem*. 269:1333–1355.
26. Smith, G., J. Wagner, and J. Keizer. 1996. Validity of the rapid buffering approximation near a point source of calcium ions. *Biophys. J.* 71:3064–3072.
27. Gillespie, D. 1976. A general method for numerically simulating the stochastic time evolution of coupled chemical reactions. *J. Comput. Phys.* 22:403–434.
28. Gonze, D., J. Halloy, and A. Goldbeter. 2002. Robustness of circadian rhythms with respect to molecular noise. *Proc. Natl. Acad. Sci. USA*. 99:673–678.
29. Bezprozvanny I., J. Watras, and B. Ehrlich. 1991. Bell-shaped calcium responses of InsP_3 - and calcium-gated channels from endoplasmic reticulum of cerebellum. *Nature*. 351:751–754.
30. Finch, E., T. Turner, and S. Goldin. 1991. Calcium as coagonist of inositol 1,4,5- trisphosphate-induced calcium release. *Science*. 252: 443–446.
31. Spät, A., P. Bradford, J. McKinney, R. Rubin, and J. Putney. 1986. A saturable receptor for ^{32}P -inositol-1,4,5-trisphosphate in hepatocytes and neutrophils. *Nature*. 319:514–516.
32. Parys, J., and I. Bezprozvanny. 1995. The inositol trisphosphate receptor of *Xenopus* oocytes. *Cell Calcium*. 18:353–363.
33. Shuai J. and P. Jung. 2002. Optimal intracellular calcium signalling. *Phys. Rev. Lett.* 88:068102-1–068102-4.
34. Li H., Z. Hou and H. Xin. 2005. Internal noise stochastic resonance for intracellular calcium oscillations in a cell system. *Phys Rev E* 71: 061916–16.
35. Skupin, A., H. Kettenmann, U. Winkler, M. Wartenberg, H. Sauer, S. Tovey, C. Taylor, and M. Falcke. 2008. How does intracellular Ca^{2+} oscillate: by chance or by the clock? *Biophys. J.* 94:2404–2411.
36. Vermassen E., J. Parys, and J.-P. Mauger. 2004. Subcellular distribution of the inositol 1,4,5-trisphosphate receptors: functional relevance and molecular determinants. *Biol. Cell*. 96:3–18.
37. Miyakawa, T., A. Maeda, T. Yamazawa, K. Hirose, T. Kurosaki, and M. Iino. 1999. Encoding of Ca^{2+} signals by differential expression of IP_3 receptor subtypes. *EMBO J.* 18:1303–1308.
38. Hattori, M., A. Suzuki, T. Higo, H. Miyauchi, T. Michikawa, T. Nakamura, T. Inoue, and K. Mikoshiba. 2004. Distinct roles of inositol 1,4,5-trisphosphate receptor types 1 and 3 in Ca^{2+} signalling. *J. Biol. Chem.* 279:11967–11975.
39. Dupont, G., and L. Combettes. 2006. Modelling the effect of specific inositol 1,4,5-trisphosphate receptor isoforms on cellular Ca^{2+} signals. *Biol. Cell*. 98:171–182.
40. Hirose, K., S. Kadowaki, M. Tanabe, H. Takeshima, and M. Iino. 1999. Spatiotemporal dynamics of inositol 1,4,5-trisphosphate that underlies complex Ca^{2+} mobilization patterns. *Science*. 284:1527–1530.
41. Young, K., M. Nash, R. Challis, and S. Nahorski. 2003. Role of Ca^{2+} feedback on single cell inositol 1,4,5-trisphosphate oscillations mediated by G-protein-coupled receptors. *J. Biol. Chem.* 278:20753–20760.
42. Sneyd, J., K. Tsaneva-Atanasova, V. Reznikov, Y. Bai, M. Sanderson, and D. Yule. 2006. A method for determining the dependence of calcium oscillations on inositol trisphosphate oscillations. *Proc. Natl. Acad. Sci. USA*. 103:1675–1680.
43. Takazawa, K., H. Passareiro, J. Dumont, and C. Erneux. 1988. Ca^{2+} /calmodulin-sensitive inositol 1,4,5-trisphosphate 3-kinase in rat and bovine brain tissues. *Biochem. Biophys. Res. Commun.* 153:632–641.
44. Shuai J., and P. Jung. 2003. Optimal ion channel clustering for intracellular calcium signalling. *Proc. Natl. Acad. Sci. USA*. 100:506–510.
45. Schipke, C., A. Heidemann, A. Skupin, O. Peters, M. Falcke, and H. Kettenmann. 2008. Temperature and nitric oxide control spontaneous calcium transients in astrocytes. *Cell Calcium*. 43:285–295.
46. Morel, J.-L., N. Fritz, J.-L. Lavie, and J. Mironneau. 2003. Crucial role of type 2 inositol 1,4,5-trisphosphate receptors for acetylcholine-induced Ca^{2+} oscillations in vascular myocytes. *Arterioscler. Thromb. Vasc. Biol.* 23:1567–1575.
47. Marhl, M., M. Gosak, G. Dixon, and A. Green. 2008. Spatio-temporal modelling explains the effect of reduced plasma membrane Ca^{2+} efflux on intracellular Ca^{2+} oscillations in hepatocytes. *J. Theor. Biol.* In press.
48. Ishii, K., K. Hirose, and M. Iino. 2006. Ca^{2+} shuttling between endoplasmic reticulum and mitochondria underlying Ca^{2+} oscillations. *EMBO Rep.* 7:390–396.
49. Huertas, M., and G. Smith. 2007. The dynamics of luminal depletion and the stochastic gating of Ca^{2+} -activated Ca^{2+} channels and release sites. *J. Theor. Biol.* 246:332–354.
50. Neher, E. 2000. Calcium buffers in flash-light. *Biophys. J.* 79:2783–2784.
51. Dargan, S., B. Schwaller, and I. Parker. 2004. Spatiotemporal patterning of IP_3 -mediated Ca^{2+} signals in *Xenopus* oocytes by Ca^{2+} -binding proteins. *J. Physiol.* 55:447–461.
52. Combettes, L., D. Tran, T. Tordjmann, M. Laurent, M. Berthon, and M. Claret. 1994. Ca^{2+} -mobilizing hormones induce sequentially ordered Ca^{2+} signals in multicellular systems of rat hepatocytes. *Biochem. J.* 304:585–594.
53. Gravecha, M., R. Toral, and J. Gunton. 2001. Stochastic effects in intercellular calcium spiking in hepatocytes. *J. Theor. Biol.* 212:111–125.
54. Prank, K., M. Waring, U. Ahlvers, A. Bader, E. Penner, M. Möller, G. Brabant, and C. Schöfl. 2005. Precision of intracellular calcium spike timing in primary rat hepatocytes. *Syst. Biol. (Stevenage)*. 2:31–34.
55. Raser, J., and E. O'Shea. 2005. Noise in gene expression: origins, consequences, and control. *Science*. 309:2010–2013.